



# Kinetic and energy production analysis of pyrolysis of lignocellulosic biomass using a three-parallel Gaussian reaction model



Tianju Chen<sup>a</sup>, Jinzhi Zhang<sup>a,b</sup>, Jinhu Wu<sup>a,\*</sup>

<sup>a</sup> Key Laboratory of Biofuels, Qingdao Institute of Bioenergy and Bioprocess Technology, Chinese Academy of Sciences, 189 Songling Road, Qingdao 266101, PR China

<sup>b</sup> University of Chinese Academy of Sciences, Beijing 100049, PR China

## HIGHLIGHTS

- Functional groups of the pseudocomponents were determined by FT-IR.
- Gaussian-DAEM-reaction model was developed for kinetic study.
- Four kinds of syngas were investigated using a three-parallel distribution model.
- The liquid production was investigated using Py-GCMS.

## ARTICLE INFO

### Article history:

Received 15 January 2016

Received in revised form 15 March 2016

Accepted 17 March 2016

Available online 23 March 2016

### Keywords:

Distributed activation energy model (DAEM)

Thermogravimetric analysis (TGA)

Kinetic analysis

Pyrolysis

## ABSTRACT

The kinetic and energy productions of pyrolysis of a lignocellulosic biomass were investigated using a three-parallel Gaussian distribution method in this work. The pyrolysis experiment of the pine sawdust was performed using a thermogravimetric–mass spectroscopy (TG–MS) analyzer. A three-parallel Gaussian distributed activation energy model (DAEM)–reaction model was used to describe thermal decomposition behaviors of the three components, hemicellulose, cellulose and lignin. The first, second and third pseudocomponents represent the fractions of hemicellulose, cellulose and lignin, respectively. It was found that the model is capable of predicting the pyrolysis behavior of the pine sawdust. The activation energy distribution peaks for the three pseudo-components were centered at 186.8, 197.5 and 203.9 kJ mol<sup>−1</sup> for the pine sawdust, respectively. The evolution profiles of H<sub>2</sub>, CH<sub>4</sub>, CO, and CO<sub>2</sub> were well predicted using the three-parallel Gaussian distribution model. In addition, the chemical composition of bio-oil was also obtained by pyrolysis–gas chromatography/mass spectrometry instrument (Py–GC/MS).

© 2016 Elsevier Ltd. All rights reserved.

## 1. Introduction

The increasing anthropogenic CO<sub>2</sub> emission and global warming have challenged the world to find new and better ways to meet the world's increasing needs for energy while reducing greenhouse gases (Lee et al., 2010). Lignocellulosic biomass is an important feedstock for the renewable production of fuels, chemicals and energy. It is one of the largest energy sources in the world. It was once an important source of energy for humankind and it is starting to play this role again (Galembeck, 2010). That is because biomass is a clean, cost-effective, CO<sub>2</sub> neutral and low sulfur content renewable material which can be used for heat and fuel production (Gordillo and Belghit, 2011). Moreover, biomass is expected to be an important source of renewable liquid transportation fuels and chemicals.

Biomass pyrolysis utilizes high temperatures to produce an economically renewable intermediate (bio-oil) that can be integrated with the existing petroleum infrastructure to produce biofuels (Mettler et al., 2012a). Bio-oil is easy to transport, making biomass a dominant choice for the replacement of fossil fuels (Mahinpey et al., 2009). Its use as fuel in boilers and engines has been tested (Chiaramonti et al., 2003a,b). In the above studies, bio-oils were obtained by decomposing biomass samples at different pyrolysis conditions and characteristics of the obtained bio-oil were also investigated by various instrumental techniques. However, the quality of bio-oil is critical to downstream process development and is determined by a number of factors like reaction timescale, extent of primary and secondary reactions, and the presence of minerals (Vinu and Broadbelt, 2012). And the storage conditions can also effect the characterizations of bio-oil (Kim et al., 2012). Pyrolysis–gas chromatography/mass spectrometry instrument (Py–GC/MS) was employed to achieve fast pyrolysis of biomass material and on-line analysis of the pyrolysis vapors. As the

\* Corresponding author.

E-mail addresses: [chentianju27@gmail.com](mailto:chentianju27@gmail.com) (T. Chen), [wujh@qibebt.ac.cn](mailto:wujh@qibebt.ac.cn) (J. Wu).

heating rate of Py-GC/MS was  $10^4 \text{ K S}^{-1}$ , the secondary reaction can be avoided (Qiang et al., 2009; Zhang et al., 2014b).

It is well known that cellulose (40–50 wt.%), hemicellulose (25–35 wt.%) and lignin (16–33 wt.%) are the building blocks of woody biomass (Vinu and Broadbelt, 2012; Zakzeski et al., 2010). Schematic representation of the location and structure of cellulose, hemicellulose and lignin in biomass material was shown in Fig. 1. Cellulose present along with hemicellulose in almost all plant cell walls. While cellulose is crystalline, strong, and resistant to hydrolysis, hemicellulose has a random, amorphous structure with little strength. Unlike cellulose, hemicellulose consists of shorter chains 500–3000 sugar units as opposed to 7000–15,000 glucose molecules per polymer seen in cellulose. In addition, hemicellulose is a branched polymer, while cellulose is unbranched. In plant cell walls, lignin fills the spaces between cellulose and hemicellulose, and it acts like a resin that holds the lignocellulose matrix together (Zakzeski et al., 2010). There are a variety of models available for analyzing the kinetics of biomass thermal decomposition studies, including first-order (Kissinger, 1956), discrete activation-energy distributions (Burnham and Braun, 1998), and sequential models (Braun and Burnham, 1987) such as models having Gaussian (Anthony and Howard, 1976), Weibull (Lakshmanan and White, 1994) and Gamma (Astarita, 1989) distributions. The distributed activation energy model (DAEM), representing the sequential models, is by far the most comprehensive model for analyzing complex reactions in thermal decomposition of biomass (Várhegyi et al., 2010). The model assumes that an infinite number of first order parallel reactions having unique kinetic parameters take place concurrently. Several researchers (Cai et al., 2013a; Li et al., 2008; Zhou et al., 2013) have investigated this kind of three parallel reaction model of biomass pyrolysis. The model assumes that lignocellulosic biomass contains three independently reacting pseudocomponents, and therefore, that the global thermal decomposition behavior reflects the individual behavior of these pseudocomponents, weighted by the composition and they also assume the DTG curve of the three pseudocomponents fitted the Gaussian distribution model. How does the char and volatile especially the  $\text{H}_2$ ,  $\text{CH}_4$ , CO and  $\text{CO}_2$  formed still a challenge for biomass pyrolysis (Mettler et al., 2012a,b).

In the previous research, the efforts focused on characterizing the bio-oil (Chen et al., 2010, 2011) and the kinetic of biomass pyrolysis (Chen et al., 2014; Zhang et al., 2014a). The main objective of the present work was to gain a better understanding of the decomposition behavior of pine sawdust using TG–MS and Py–GCMS. The multi-Gaussian-DAEM-reaction model was used to investigate the kinetic of pine sawdust. The trends of light gases

( $\text{H}_2$ ,  $\text{CH}_4$ , CO and  $\text{CO}_2$ ) with the increase of the temperature were also studied. This study may provide a useful reference for energy carriers from the pyrolysis of biomass.

## 2. Methods

### 2.1. Materials and methods

The pine sawdust was used as the typical raw biomass material in this study. The proximate and ultimate analyses of the samples are listed in Table 1. Cellulose (CAS: 9004-34-6, product number: C6288) and lignin (CAS: 8068-05-1, product number: 471003) were bought from Sigma–Aldrich Co., Ltd (USA). Cellulose was a polysaccharide composed of long chains of  $\beta(1,4)$  linked D-glucose units. The low sulfonate content alkali lignin was chosen in this study. In this work, xylan (CAS: 9014-63-5, product number: X4252) was purchased from Sigma–Aldrich Co., Ltd. All samples were dried for 12 h at 378 K to remove water before the TGA experiment. Prior to the experiment, the samples were dried in an electrically heated oven at the temperature of 378 K for 12 h and stored in air-tight bags until experimentation.

### 2.2. Fourier-transform infrared (FT-IR) analysis

The FT-IR analysis was used to determine the functional groups of the biomass material. Four kinds of raw material including pine sawdust, cellulose, hemicelluloses and lignin were analyzed in this work. The raw material was mixed with KBr powder which had been dried at  $105^\circ\text{C}$  at a ratio of 3 mg raw material: 1000 mg KBr for all samples. The powder mixture was then re-ground in a mortar and pestle to ensure homogeneity and was stored in a desiccator. Pellets were created using 150–250 mg of powder in a pellet press at 10 Mpa of pressure. Using a Mattson Model 5020 FT-IR Spectrometer (Madison, WI) at wave numbers from 400 to  $4000 \text{ cm}^{-1}$ , each sample was scanned 100 times, with a resolution of  $0.4 \text{ cm}^{-1}$ , subtracting a blank value obtained from a pure KBr pellet.

### 2.3. TG–MS analysis

The experiments were performed using a thermogravimetric analyzer (TGA, TA Instruments Q600) with a MS (Thermo star, Pfeiffer), operating at the heating rate of  $50 \text{ K min}^{-1}$ . A thin layer of the sample (ca. 10 mg) was distributed evenly in a ceramic crucible and placed in the TGA. The sample was then heated at a desired heating rate to the final temperature of 1273 K. The

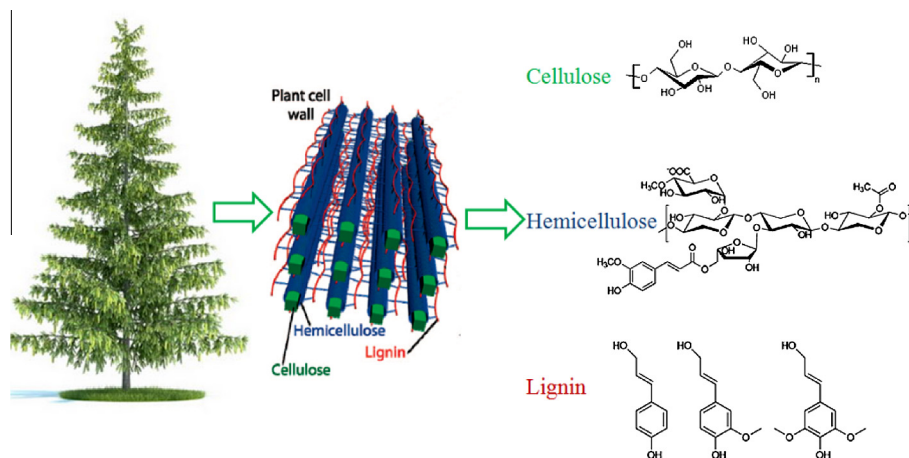


Fig. 1. Schematic representation of the location and structure of cellulose, hemicellulose and lignin in biomass material.

**Table 1**

The proximate and ultimate analyses of pine sawdust.

Proximate analysis (wt.%)		Elemental analysis	
Moisture	7.59	Carbon	48.42
Volatiles	77.28	Hydrogen	5.51
Fixed carbon	14.28	Nitrogen	0.08
Ash	0.85	Oxygen <sup>a</sup>	45.14

<sup>a</sup> By difference.

reaction of such a thin layer of sample could be considered kinetically controlled without incurring any significant mass and heat transfer limitations of concern (Simmons and Gentry, 1986). During the heating, the mass and temperature of the sample were simultaneously and continuously recorded. In the pyrolysis experiments, Helium of ultra high purity was passed through the TGA at a constant flow rate of 100 ml min<sup>-1</sup> to provide the inert gas environment and to sweep away the volatile released.

#### 2.4. Py-GC/MS analysis

Py-GC/MS experiment was performed in the CDS Pyroprobe 5200 HP pyrolyser (Chemical Data Systems) connected with a gas chromatography/mass spectrometry (7890/5975C, Agilent). During the experiments, the pyrolysis tube was filled with 0.5 mg of sawdust. The pyrolysis temperature was set at 500 °C with a heating rate of 20 °C ms<sup>-1</sup> and held for 25 s. A helium carrier gas of 30 ml min<sup>-1</sup> flow rate was used to purge the pyrolysis chamber. The chromatographic separation of the volatile products was performed using an Agilent HP-5 capillary column. Helium (99.999%) was used as the carrier gas with a constant flow rate of 1 ml min<sup>-1</sup> and a 1:100 split ratio. The oven temperature was programmed from 40 to 180 °C with the heating rate of 4 °C min<sup>-1</sup>, and then to 280 °C with the heating rate of 10 °C min<sup>-1</sup>. The temperature of the GC/MS interface was held at 280 °C. The mass spectra were obtained from *m/z* 50 to 400. The chromatographic peaks were identified according to the NIST library.

#### 2.5. Distributed activation energy model

DAEM is a multiple parallel reaction process, which assumes the pyrolysis mechanism of solid fuels is made up of an infinite number of independent, parallel, first order reactions with unique activation energies (Miura, 1995). The DAEM equation is given as Eq. (1):

$$\alpha(T) = \int_0^\infty \left\{ 1 - \exp \left[ -\frac{k_0}{\beta} \int_0^T \exp \left( -\frac{E}{RT} \right) dT \right] \right\} f(E) dE \quad (1)$$

where  $\alpha(T)$  is extent of conversion,  $T$  is the absolute temperature,  $k_0$  is the pre-frequency factor (frequency factor),  $\beta$  is the heating rate,  $E$  is the activation energy,  $R$  is the universal gas constant, and  $f(E)$  is the activation energy distribution.

In order to estimate the values of kinetic parameters, the activation energy distribution is generally assumed by a Gaussian distribution with mean activation energy  $E_0$  and standard deviation  $\sigma$  is shown as Eq. (2):

$$f(E) = \frac{1}{\sigma\sqrt{2\pi}} \exp \left[ -\frac{(E-E_0)^2}{2\sigma^2} \right] \quad (2)$$

The derivative of Eq. (1) is expressed as:

$$\frac{d\alpha(T)}{dT} = \frac{1}{\sigma\sqrt{2\pi}} \int_0^\infty \frac{k_0}{\beta} \exp \left[ -\frac{E}{RT} - \frac{k_0}{\beta} \int_0^T \exp \left( -\frac{E}{RT} \right) dT - \frac{(E-E_0)^2}{2\sigma^2} \right] dE \quad (3)$$

In order to optimize values of kinetic parameters ( $k_0$ ,  $E_0$  and  $\sigma$ ) in Eq. (3), the objective function (the fitting quality, *Fit*) is defined according to the equation shown below:

$$Fit(\%) = 100 \times \frac{\sqrt{\frac{S}{n_d}}}{\left( \frac{d\alpha}{dT} \right)_{\max}} \quad (4)$$

$$S = \sum_{i=1}^{n_d} \left[ \left( \frac{d\alpha}{dT} \right)_{\exp,i} - \left( \frac{d\alpha}{dT} \right)_{\text{cal},i} \right]^2 \quad (5)$$

where  $n_d$  represents the number of the data points,  $(d\alpha/dT)_{\max}$  is the maximum experimental value, and  $(d\alpha/dT)_{\text{cal}}$  represents those calculated by Gaussian DAEM model for a given set of parameters of  $k_0$ ,  $E_0$  and  $\sigma$ ,  $(d\alpha/dT)_{\exp}$  is the experimental data, and  $(d\alpha/dT)_{\text{cal}}$  represents those calculated by Eq. (3) for a given set of parameters of  $E_0$  and  $\sigma$ .

### 3. Results and discussion

#### 3.1. Chemical structure analysis of lignocellulose biomass

The chemical structure of the pine sawdust and the three components were analyzed using Fourier-transform infrared (FT-IR) spectroscopy throw pelleting the sample with KBr powder. The typical functional groups and the IR signal with the possible compounds of cellulose, hemicelluloses, lignin and pine sawdust are listed in Table 2. It can be seen that the cellulose, hemicelluloses, lignin and pine sawdust are most likely consisted of alkene, esters, aromatics, ketone and alcohol, with different oxygen-containing functional groups observed, e.g., O–H (3500–3200 cm<sup>-1</sup>), C–O–C (1270–1250 cm<sup>-1</sup>), C–O–H (ca 1050 cm<sup>-1</sup>), etc. Still, they showed different IR structures. The highest IR absorbance of O–H was found with cellulose while hemicelluloses contained the highest C–O compounds. Compared with cellulose and hemicelluloses, a bit difference was found in the finger region (1592–1043 cm<sup>-1</sup>) for lignin's IR spectra. While for lignocellulosic biomass material, the pine sawdust contain all the IR spectra that in cellulose, hemicelluloses and lignin.

#### 3.2. Kinetic study of lignocellulosic biomass pyrolysis

The thermal properties of pine sawdust pyrolysis were shown in Fig. 2. According to the results of TG and DTG curves of pine sawdust pyrolysis as shown in Fig. 2(a), the main decomposition temperature of pine sawdust is ranging from 500 to 850 K. About 16 wt.% solid residue was remaining. In the pyrolysis process, the biochar can be formed from the polycondensation of biomass.

**Table 2**

The main functional groups identified by FTIR.

Functional group	Position			
	Cellulose	Hemicellulose	Lignin	Pine sawdust
OH stretching	3431	3420	3475	3439
CH stretching of methylene	2918	2919	2919	2919
O–H bending of adsorbed water	1632	1573	1592	1636
C=C stretching in aromatic ring	–	–	1513	1511
CH scissoring	1416	1416	1450	1425
C–OH in plane bending	1371	–	1384	1375
C–O stretching phenol	–	–	1269	1267
C–O stretching in primary alcohol	1060	1046	1043	1058
CH <sub>2</sub> swing in alkene	–	890	–	890

The reaction rate is measurable above 450 K, and the pyrolysis is essentially complete at 950 K. So the investigated temperature range is 450–950 K. The DTG curve shows a peak at 667 K. The peak can be attributed to the decomposition of cellulose. To the left of the maxima, the DTG peak shows a shoulder at 625 K. This shoulder is associated with the pyrolysis of hemicellulose. A slow, flat tailing of the peak in the upper part of the temperature domain was observed, which was probably mainly associated with the decomposition of lignin.

Lignocellulosic biomass contains three main components: hemicellulose, cellulose, and lignin. The pyrolysis kinetics of these

components can be described well by using the DAEM. A model consisting of three parallel DAEM reactions was assumed to describe the pyrolysis kinetics of lignocellulosic biomass. In this model, the lignocellulosic biomass is regarded as a sum of three pseudo-components: hemicellulose, cellulose, and lignin. It is further assumed that there is no interaction among these pseudo-components and the pyrolysis kinetics of each pseudo-component can be described by using the DAEM. The equation for the three-parallel-DAEM-reaction model is given in Eq. (6). In this equation,  $-d\alpha/dT$  is the reaction rate obtained from the DTG curve of biomass pyrolysis,  $d\alpha_j(T)/dT$  is the conversion rate of the  $j$ th pseudo-component which can be described by Eq. (3),  $c_j$  represents the fraction of volatiles produced by the  $j$ th pseudo-component.

$$\frac{d\alpha}{dT} = \sum_{j=1}^n c_j \frac{d\alpha_j}{dT} \quad (6)$$

The three-parallel-DAEM-reaction model was used to describe the pyrolysis kinetics of lignocellulosic biomass feedstocks. Fig. 2(b) showed the comparison between the experimental DTG curves and the data predicted by the three-parallel-DAEM-reaction model. The residuals between the observed and calculated data are plotted underneath the figure. Fig. 2(b) also showed the good fitness of the model to the experimental results. The  $Fit(\%)$  was 5.4 and the  $R^2$  was 0.982. The shape and position of the three pseudo-components were similar to the hemicellulose, cellulose and lignin. The major portion of the hemicellulose and cellulose reacts in a relatively narrow range of low temperatures. The third pseudo-component represents the sum of the remaining amounts of these components plus the fractions of lignin, which decomposes in a broad temperature range. The weight loss rate of the three pseudo-components can be calculated through the integrate of the DTG curve as shown in Fig. 2(c). As shown in Fig. 2(c), the weight loss rate for the hemicelluloses, cellulose and lignin is about 52%, 26% and 22%.

The  $f(E)$  curves for hemicellulose, cellulose and lignin were shown in Fig. 3, it can be seen that the activation energies changed from 130 to 275 kJ mol<sup>-1</sup>. Gaussian distribution of activation energy was widely used for biomass thermal decompositions. Cai et al. (2013b) reported that the activation energy values for solid-state reactions were between 50 and 350 kJ mol<sup>-1</sup>, indicating that the activation energy distribution in this study was reasonable. As shown in Fig. 3, the activation energy for hemicellulose, cellulose and lignin were 186.8, 197.5 and 203.9 kJ mol<sup>-1</sup>. The  $\sigma$

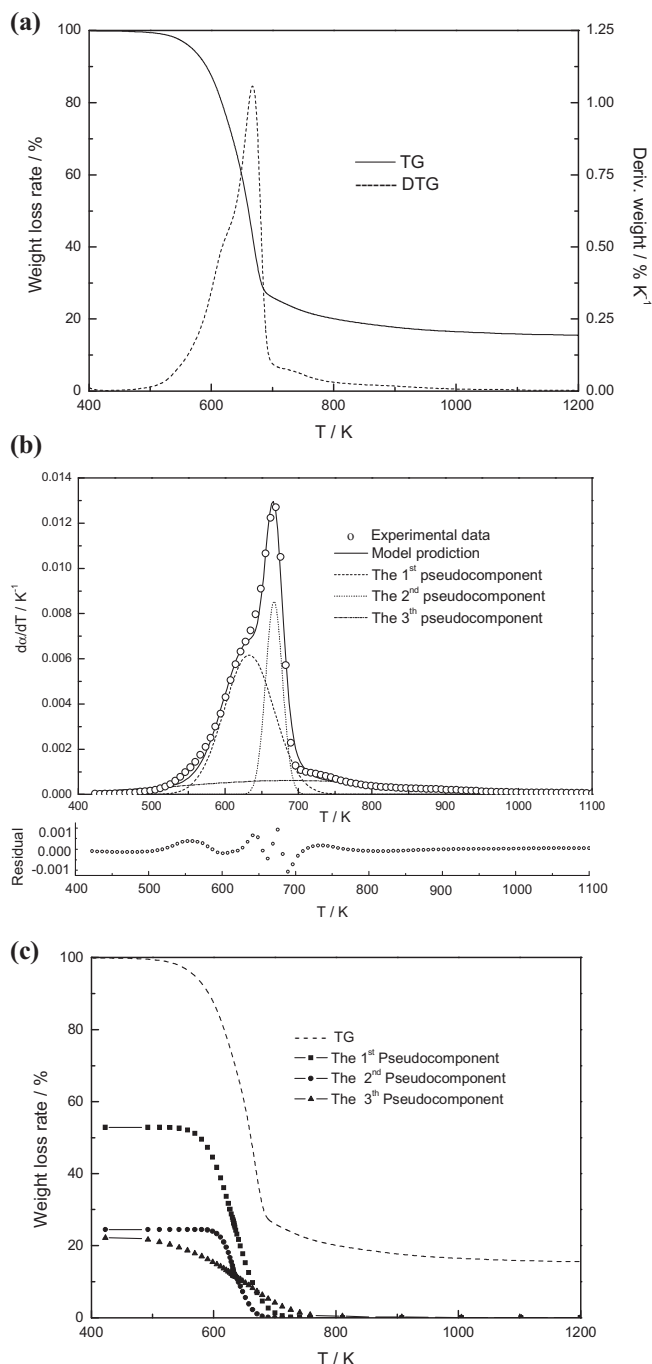


**Fig. 2.** The thermal properties of pine sawdust pyrolysis: (a) TG and DTG curves, (b) experimental and calculated conversion rate curves of pine sawdust (the residuals between the experimental data and the model prediction data are plotted underneath the figure), (c) the weight loss rate of the three pseudocomponents.

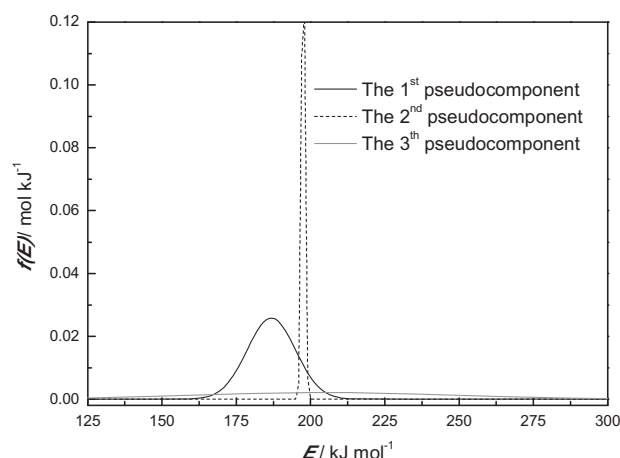


**Fig. 3.** Activation energy distributions of three pseudocomponents for pine sawdust sample.



of hemicellulose, cellulose and lignin were 8.16, 0.58 and 4.31 kJ mol<sup>-1</sup>, respectively. It was concluded that the activation energies required to decompose different intermediate products were similar for one pseudocomponent. Increasing the Gaussian distribution parameter ( $\sigma$ ) makes the  $f(E)$  profile broader. The decomposition of hemicellulose and lignin both occurred in a wide temperature range, and therefore the interval of activation energy was larger than cellulose.

### 3.3. Evolution of light gases

The syngas from pyrolysis of biomass is useful if the combustible gases of CO, H<sub>2</sub> and CH<sub>4</sub> contents are high. The literature (Chen et al., 2010) has reported that syngas can be used as a heat source in a recycling fluidized-bed reactor. The ions of 2, 16, 28 and 44 m/z assigned to H<sub>2</sub>, CH<sub>4</sub>, CO and CO<sub>2</sub> were detected for pine sawdust degradation under inert atmosphere. Three-parallel reaction model was used to investigate the evolution of H<sub>2</sub>, CH<sub>4</sub>, CO and CO<sub>2</sub>. Curves of evolution of light gases based on three-parallel reaction model are shown in Fig. 4. For the lignocelluloses biomass material, the H<sub>2</sub>, CH<sub>4</sub>, CO and CO<sub>2</sub> were measurable above the temperature of 550, 525, 510 and 500 K, respectively. The oxygen content of pine sawdust is 45.14 wt.% and the chemical bond energy of C–O bond (326 kJ mol<sup>-1</sup>) is lower than C–H bond (414 kJ mol<sup>-1</sup>) and C–C bond (332 kJ mol<sup>-1</sup>) (Luo, 2004). That is why the H<sub>2</sub> content was detected at the highest temperature.

According to the results in Fig. 4, the three-parallel reaction model can fit the experimental data very well. The evolution of light gases from the three pseudocomponents was shown based on three-Gaussian-parallel reaction model. The results vividly showed that the evolution of light gases from hemicellulose, cellulose and lignin. The peak of the evolution of H<sub>2</sub>, CH<sub>4</sub>, CO and

CO<sub>2</sub> is about 640–660 K, which is almost the same as the DTG curve of pine sawdust. The evolution of H<sub>2</sub>, CH<sub>4</sub>, CO and CO<sub>2</sub> from hemicellulose had a relative lower reaction temperature compared with cellulose and lignin. Hemicellulose has a lower thermal stability than cellulose and lignin. The temperature range of H<sub>2</sub>, CH<sub>4</sub>, CO and CO<sub>2</sub> evolution from cellulose pyrolysis is 650–750 K. For the lignin pyrolysis, the evolution of CH<sub>4</sub>, CO and CO<sub>2</sub> showed a lone peak. But for the evolution of H<sub>2</sub>, only a small peak was showed in Fig. 4(a). The evolution of H<sub>2</sub> from lignin pyrolysis lags behind CH<sub>4</sub>, CO and CO<sub>2</sub>. In our previous research (Chen et al., 2016), the main syngas contents of CH<sub>4</sub>, H<sub>2</sub>, CO and CO<sub>2</sub> were investigated from the pyrolysis of biomass material. The results showed that the content of combustible gases were more than 60%. At first, the contents of CO and CO<sub>2</sub> were about 95%. While the contents of H<sub>2</sub> and CH<sub>4</sub> increased with time. These results indicated that in the biomass pyrolysis process, the evolution of H<sub>2</sub> and CH<sub>4</sub> lags behind CO and CO<sub>2</sub>. For one thing, the chemical bond energy of C–O (335 kJ mol<sup>-1</sup>) and C–C (332 kJ mol<sup>-1</sup>) bond is lower than C–H bond (414 kJ mol<sup>-1</sup>). For another thing, lignin is a more stable polymer material, more than 60 wt.% of lignin can form biochar at the temperature of 1000 K (Zhang et al., 2014a).

### 3.4. Py-GC/MS analysis

Py-GC/MS experiment was conducted to further investigate the chemical compounds production from fast pyrolysis of pine sawdust. The detailed main pyrolytic productions and their relative mass contents of pine sawdust are shown in Table 3. The compounds were ordered according to their retention times. When the peak areas and relative abundance were compared in terms of area percentage, it was found that 46 types of chemical compounds were detected. The main productions are Acids, Furfurals

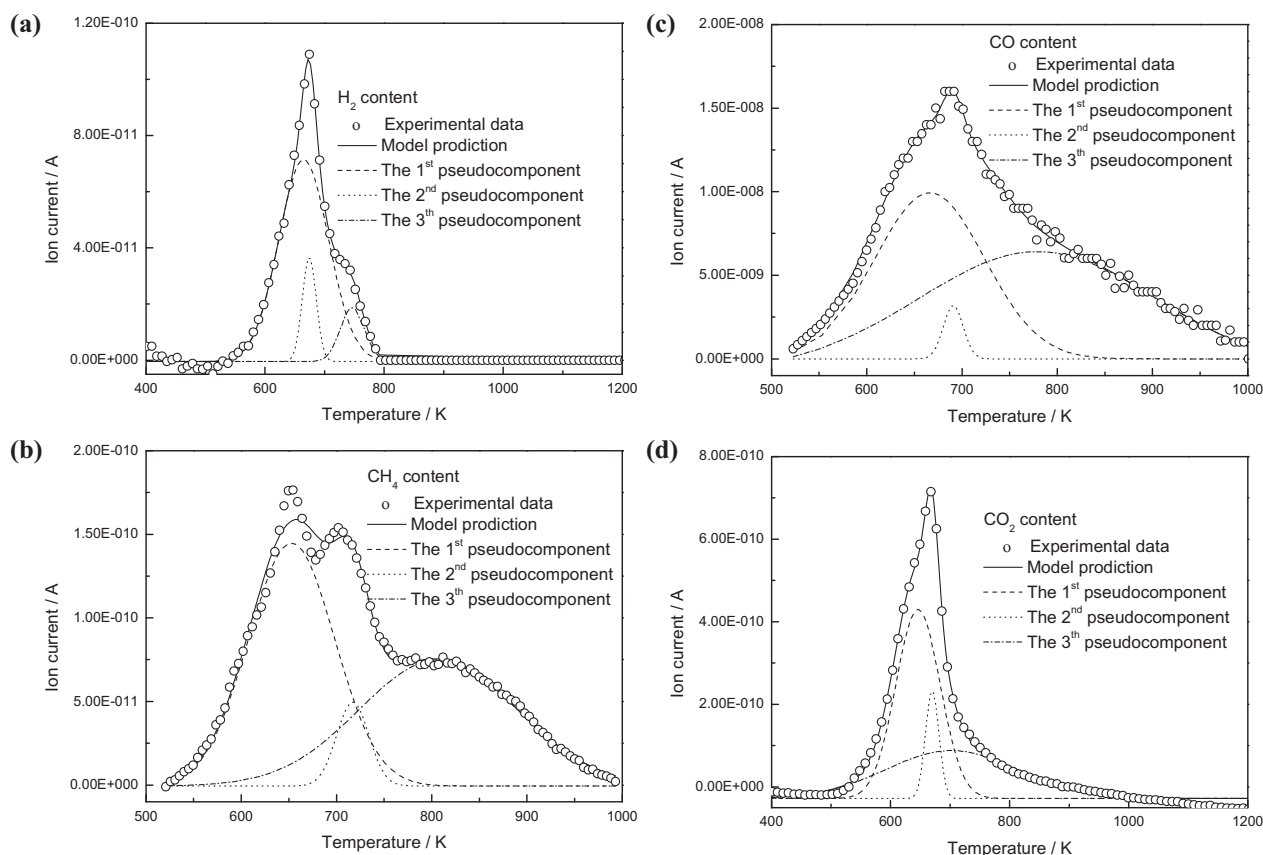


Fig. 4. Curves of evolution of light gases based on three-parallel reaction model: (a) H<sub>2</sub>; (b) CH<sub>4</sub>; (c) CO; (d) CO<sub>2</sub>.

**Table 3**

Main pyrolytic productions and their relative mass contents of pine sawdust.

Peak No.	Main identified compounds	RTA (min)	Mol. mass	Relative mass content (%)
1	Isobutane	1.166	58	1.62
2	Acetic acid	1.429	60	21.70
3	1-Hydroxy-2-propanone	1.738	74	4.41
4	2-Methyl-(E)-2-butenal	2.632	84	0.86
5	Acetic acid-methyl ester	2.941	74	2.60
6	Propanal	3.119	58	1.48
7	2-Oxo-methyl ester-propanoic acid	3.296	102	1.56
8	Furfural	4.112	96	1.41
9	2-Furanmethanol	4.631	98	0.83
10	2(5H)-Furanone	5.723	84	1.71
11	1,2-Cyclopentanedione	5.927	98.037	1.87
12	5-Methyl-2-furancarboxaldehyde	6.663	110	0.44
13	2H-Pyran-2,6(3H)-dione	7.242	112	0.53
14	Dihydro-2,4(1H,3H)-pyrimidinedione	7.288	114	1.76
15	2-Cyclopenten-1-one,2-hydroxy-3-methyl	7.807	112	0.61
16	4-Methyl-5H-furan-2-one	8.11	98	0.73
17	5,6-Epoxyhexanol-1	8.346	116	1.33
18	4-Methyl-phenol	8.695	108	0.63
19	2-Methoxy-phenol	8.853	124	2.91
20	N-methyl-1,3-propanediamine	8.918	88	0.93
21	1,4-dioxaspiro[2.4]heptan-5-one	9.405	114	0.93
22	Barbituric acid	9.859	128	0.63
23	2-Oxo-butanoic acid	10.155	102	0.81
24	2,3,4-Trimethyl-hexane	10.358	128	1.32
25	2-Methoxy-4-methyl-phenol	10.477	138	3.78
26	1,2-Benzenediol	10.713	110	1.23
27	2,3-Anhydro-D-mannosan	10.957	144	0.33
28	5-(Hydroxymethyl)-2-furancarboxaldehyde	11.036	126	1.52
29	3-Buten-1-yl ethenyl sulfide	11.522	114	0.68
30	4-Ethyl-2-methoxy-phenol	11.726	152	0.80
31	2-Ethenyl-4-methyl-1,3-dioxolane	12.048	114	1.80
32	2-Methoxy-4-vinyl phenol	12.213	150	4.36
33	Eugenol	12.798	164	1.08
34	2-Methoxy-4-propyl-phenol	12.929	166	0.65
35	Vanillin	13.35	152	1.45
36	2-Methoxy-4-(1-propenyl)-(E)-phenol	13.462	164	4.20
37	2-Methoxy-4-propyl-phenol	14.119	166	0.71
38	1-(2,4,5-Trimethylphenyl)-ethanone	14.336	162	0.33
39	1-(4-Hydroxy-3-methoxyphenyl)-ethanone	14.455	166	3.75
40	D-Allose	14.586	180	14.57
41	1-(4-Isopropoxy-3-methoxyphenyl)-propan-2-one	15.001	222	0.49
42	4-(3-Hydroxy-1-propenyl)-2-methoxy-phenol	15.52	180	0.33
43	1,6-Anhydro-beta-D-glucofuranose	15.776	162	0.67
44	Benzeneacetic acid, 4-hydroxy-3-methoxy	16.355	182	1.01
45	4-Hydroxy-2-methoxycinnamaldehyde	17.295	178	2.08
46	n-Hexadecanoic acid	19.557	256	0.59

and Phenols. It is known that the chemical compounds have a higher commercial value. From the structure of cellulose, hemicellulose and lignin as shown in Fig. 1, the chemical compounds of Acid, Furans, Furfural, Neutral sugars and Phenols are the main productions from the pyrolysis of cellulose (Mettler et al., 2012a) and hemicellulose (Wang et al., 2015). The lignin is a rich source of phenolic compounds. It is considered that phenolic compounds are predominantly produced by degradation of lignin (Custodis et al., 2015).

#### 4. Conclusions

A three-parallel-DAEM model was used to predict the pyrolysis behavior of the pine sawdust and the pyrolysis kinetics. The activation energy distributions obtained were in the ranges of 186.8, 197.5 and 203.9 kJ mol<sup>-1</sup> for the three components, namely, hemicelluloses, cellulose and lignin, respectively. The experimental evolutions of H<sub>2</sub>, CH<sub>4</sub>, CO and CO<sub>2</sub> matched with the calculated results very well, suggesting that model is able to predict the gaseous products of pyrolysis. There were 46 types of chemical compounds were detected for the Py-GCMS of pine sawdust. The main chemical compounds are acids and phenolics.

#### Acknowledgements

Financial support from National Natural Science Foundation of China (Project No. 51406220) is greatly acknowledged. In addition, Dr. Mingming Zhu from The University of Western Australia is greatly acknowledges for his valuable suggestions and review of the manuscript.

#### Appendix A. Supplementary data

Supplementary data associated with this article can be found, in the online version, at <http://dx.doi.org/10.1016/j.biortech.2016.03.091>.

#### References

- Anthony, D.B., Howard, J.B., 1976. Coal devolatilization and hydrogastification. *AIChE J.* 22, 625–656.
- Astarita, G., 1989. Lumping nonlinear kinetics: apparent overall order of reaction. *AIChE J.* 35, 529–532.
- Braun, R.L., Burnham, A.K., 1987. Analysis of chemical reaction kinetics using a distribution of activation energies and simpler models. *Energy Fuels* 1, 153–161.

- Burnham, A.K., Braun, R.L., 1998. Global kinetic analysis of complex materials. *Energy Fuels* 13, 1–22.
- Cai, J., Wu, W., Liu, R., 2013a. Sensitivity analysis of three-parallel-DAEM-reaction model for describing rice straw pyrolysis. *Bioresour. Technol.* 132, 423–426.
- Cai, J., Wu, W., Liu, R., Huber, G.W., 2013b. A distributed activation energy model for the pyrolysis of lignocellulosic biomass. *Green Chem.* 15, 1331–1340.
- Chen, T., Deng, C., Liu, R., 2010. Effect of selective condensation on the characterization of bio-oil from pine sawdust fast pyrolysis using a fluidized-bed reactor. *Energy Fuels* 24, 6616–6623.
- Chen, T., Liu, R., Scott, N.R., 2016. Characterization of energy carriers obtained from the pyrolysis of white ash, switchgrass and corn stover — biochar, syngas and bio-oil. *Fuel Process. Technol.* 142, 124–134.
- Chen, T., Wu, C., Liu, R., Fei, W., Liu, S., 2011. Effect of hot vapor filtration on the characterization of bio-oil from rice husks with fast pyrolysis in a fluidized-bed reactor. *Bioresour. Technol.* 102, 6178–6185.
- Chen, T., Wu, J., Zhang, J., Wu, J., Sun, L., 2014. Gasification kinetic analysis of the three pseudocomponents of biomass-cellulose, semicellulose and lignin. *Bioresour. Technol.* 153, 223–229.
- Chiaromonti, D., Bonini, M., Fratini, E., Tondi, G., Gartner, K., Bridgwater, A.V., Grimm, H.P., Soldaini, I., Webster, A., Baglioni, P., 2003a. Development of emulsions from biomass pyrolysis liquid and diesel and their use in engines—part 1: emulsion production. *Biomass Bioenergy* 25, 85–99.
- Chiaromonti, D., Bonini, M., Fratini, E., Tondi, G., Gartner, K., Bridgwater, A.V., Grimm, H.P., Soldaini, I., Webster, A., Baglioni, P., 2003b. Development of emulsions from biomass pyrolysis liquid and diesel and their use in engines—part 2: tests in diesel engines. *Biomass Bioenergy* 25, 101–111.
- Custodis, V.B.F., Bährle, C., Vogel, F., van Bokhoven, J.A., 2015. Phenols and aromatics from fast pyrolysis of variously prepared lignins from hard- and softwoods. *J. Anal. Appl. Pyrolysis* 115, 214–223.
- Galembeck, F., 2010. Synergy in food, fuels and materials production from biomass. *Energy Environ. Sci.* 3, 393–399.
- Gordillo, E.D., Belghit, A., 2011. A bubbling fluidized bed solar reactor model of biomass char high temperature steam-only gasification. *Fuel Process. Technol.* 92, 314–321.
- Kim, T.-S., Kim, J.-Y., Kim, K.-H., Lee, S., Choi, D., Choi, I.-G., Choi, J.W., 2012. The effect of storage duration on bio-oil properties. *J. Anal. Appl. Pyrolysis* 95, 118–125.
- Kissinger, H.E., 1956. Variation of peak temperature with heating rate in differential thermal analysis. *J. Res. Nat. Bureau Stand.* 57, 217–221.
- Lakshmanan, C.C., White, N., 1994. A new distributed activation energy model using Weibull distribution for the representation of complex kinetics. *Energy Fuels* 8, 1158–1167.
- Lee, J.W., Hawkins, B., Day, D.M., Reicosky, D.C., 2010. Sustainability: the capacity of smokeless biomass pyrolysis for energy production, global carbon capture and sequestration. *Energy Environ. Sci.* 3, 1695–1705.
- Li, Z., Zhao, W., Meng, B., Liu, C., Zhu, Q., Zhao, G., 2008. Kinetic study of corn straw pyrolysis: comparison of two different three-pseudocomponent models. *Bioresour. Technol.* 99, 7616–7622.
- Luo, Y.R., 2004. Handbook of Bond Dissociation Energies in Organic Compounds. *Journal of the American Chemical Society JACS*, 126.
- Mahinpey, N., Murugan, P., Mani, T., Raina, R., 2009. Analysis of bio-oil, biogas, and biochar from pressurized pyrolysis of wheat straw using a tubular reactor. *Energy Fuels* 23, 2736–2742.
- Mettler, M.S., Mushrif, S.H., Paulsen, A.D., Javadekar, A.D., Vlachos, D.G., Dauenhauer, P.J., 2012a. Revealing pyrolysis chemistry for biofuels production: conversion of cellulose to furans and small oxygenates. *Energy Environ. Sci.* 5, 5414–5424.
- Mettler, M.S., Vlachos, D.G., Dauenhauer, P.J., 2012b. Top ten fundamental challenges of biomass pyrolysis for biofuels. *Energy Environ. Sci.* 5, 7797–7809.
- Miura, K., 1995. A new and simple method to estimate  $f(E)$  and  $k_0(E)$  in the distributed activation energy model from three sets of experimental data. *Energy Fuels* 9, 302–307.
- Qiang, L., Wen-zhi, L., Dong, Z., Xi-feng, Z., 2009. Analytical pyrolysis–gas chromatography/mass spectrometry (Py–GC/MS) of sawdust with Al/SBA-15 catalysts. *J. Anal. Appl. Pyrolysis* 84, 131–138.
- Simmons, G.M., Gentry, M., 1986. Particle size limitations due to heat transfer in determining pyrolysis kinetics of biomass. *J. Anal. Appl. Pyrolysis* 10, 117–127.
- Várhegyi, V.B., Bobály, B.Z., Jakab, E., Chen, H., 2010. Thermogravimetric study of biomass pyrolysis kinetics. A distributed activation energy model with prediction tests. *Energy Fuels* 25, 24–32.
- Vinu, R., Broadbelt, L.J., 2012. A mechanistic model of fast pyrolysis of glucose-based carbohydrates to predict bio-oil composition. *Energy Environ. Sci.* 5, 9808–9826.
- Wang, S., Ru, B., Dai, G., Sun, W., Qiu, K., Zhou, J., 2015. Pyrolysis mechanism study of minimally damaged hemicellulose polymers isolated from agricultural waste straw samples. *Bioresour. Technol.* 190, 211–218.
- Zakzeski, J., Bruijninx, P.C.A., Jongerius, A.L., Weckhuysen, B.M., 2010. The catalytic valorization of lignin for the production of renewable chemicals. *Chem. Rev.* 110, 3552–3599.
- Zhang, J., Chen, T., Wu, J., Wu, J., 2014a. Multi-Gaussian-DAEM-reaction model for thermal decompositions of cellulose, hemicellulose and lignin: comparison of  $N_2$  and  $CO_2$  atmosphere. *Bioresour. Technol.* 166, 87–95.
- Zhang, X., Sun, L., Chen, L., Xie, X., Zhao, B., Si, H., Meng, G., 2014b. Comparison of catalytic upgrading of biomass fast pyrolysis vapors over CaO and Fe(III)/CaO catalysts. *J. Anal. Appl. Pyrolysis* 108, 35–40.
- Zhou, H., Long, Y., Meng, A., Li, Q., Zhang, Y., 2013. The pyrolysis simulation of five biomass species by hemi-cellulose, cellulose and lignin based on thermogravimetric curves. *Thermochim. Acta* 566, 36–43.